Available online at www.sciencedirect.com

SciVerse ScienceDirect

Energy Procedia 14 (2012) 2088 – 2095

Energy Procedia

2nd ICAEE: 27-28 December 2011, Bangkok, Thailand

A Fluid-Thermo-Electric Coupled Field Analysis of a Novel Integrated Thermoelectric Device

B. V. K. Reddy, Matthew Barry, John Li, Minking K. Chyu*

Department of Mechanical Engineering and Materials Science, University of Pittsburgh, Pittsburgh, PA 15261, USA

Abstract

Thermoelectric elements made of semiconductor plates laminated with a highly electrically and thermally conducting inter-connector with a flow channel configuration can be treated as integrated Thermoelectric Device (TED). Elements with constructed bulk crystalline n-type and p-type (Bismuth-Telluride-Selenium) semiconducting materials and copper as a conducting material are considered. In this study, the thermoelectric performance of such an element using fluid-thermo-electric coupled field numerical methods has been investigated. The TED is subjected to constant cold temperature at the bottom and top surfaces while the inter-connector channel walls are exposed to hot fluid flow; the remaining surfaces are kept adiabatic. The performance of the integrated TED element is studied in terms of power output P_0, heat input Q_h, conversion efficiency η and produced electric voltage V for different load resistances R_L, inlet hot fluid temperatures T_{in} and flow rates Re_{Dh}. For a fixed T_{in}, optimum η is shown at a load resistance R_L which is slightly lesser than total internal resistance R_{in} value. An increase in T_{in} results in an enhancement in P_0 and η, however, it has a minimal effect on the variation of optimum load resistance R_{optmL}. At higher T_{in} values, the increment in R_L showed a significant change in the heat input Q_h values. The Re_{Dh} had a prominent effect on TED performance predictions. The P_0 increased nearly three-fold at $Re_{Dh} = 500$ in comparison to $Re_{Dh} = 100$. It is recommended that for an accurate modeling, design and optimization of state-of-the-art TED with flow channels to be carried out using fluid-thermo-electrical coupling field simulations.

Thermoelectrics; Integrated; Flow channel; Numerical model; Performance; Waste heat recovery

1. Introduction

Thermoelectric device (TED) is made by joining two dissimilar, electrically conductive materials. TED operates based on the principles of Seebeck and Peltier effects. Utilizing the Seebeck effect, TED acts as a power generator when the two junctions are exposed to temperature differential. The TED then generates a voltage potential, known as the Seebeck voltage. Similarly, TED works as a refrigerator when electric current applied across the element creates a temperature differential at the material junctions, known as the Peltier effect [1]. These devices have neither moving parts nor emit noise pollution and are also environmental friendly. TEDs have a wide range of applications include temperature measurement, power sources in oil and natural gas facilities, remote radio and satellite power generation stations, refrigeration cooling and waste heat recovery systems.

It is estimated that nearly 70% of the fuel energy in automobiles, power plants and industrial systems is rejected to surroundings as a waste heat. A reliable technology for effectively converting waste heat into useful energy, i.e. electricity is TEDs. Conventional cascading and segmented TEDs are the primary methods for extracting waste heat from low and high temperature sources. In [2], they developed a segmented TED using novel p-type Zn_4Sb_3 and $CeFe_4Sb_{14}$, and n-type $CoSb_3$ based alloys, which operates over a temperature range of 300-973 K. They achieved a conversion efficiency of 15%. Recently, [3] studied using a one-dimensional thermal resistance model for thermoelectric modules with

* Corresponding author. Tel.: +1-412-624-9720 fax: +1-412-624-4846.
E-mail address: mkchyu@pitt.edu

doi:10.1016/j.egypro.2011.12.1212

applications to waste heat recovery from an automobile engine and compared their model with experimental data. The results showed that the performance of a module on the exhaust pipe performs better compared to a module on the radiator system.

Most of the studies dealt with one-dimensional models, even though electric field and temperature distributions are multidimensional in TEDs. However, in a few articles [4,5], they demonstrated that the three-dimensional simulations are more accurate in modeling, design and optimization of TEDs. The authors [4] showed that the electric power produced is sensitive to hot fluid properties and significantly depends on real operating conditions, but at present is inefficient if one considers the weight to power ratio. In [5], they proposed and implemented a non-linear fluid-thermal-electric three-dimensional numerical model for thermoelectric generators in FLUENT-UDS (User Defined Scalar) environment.

Although conventional TED designs are applicable to waste heat recovery operations, they require large amount of rare earth materials for module fabrication. These designs also induce large amounts of thermal stresses due to their structure. Furthermore, there exist substantial thermal resistances among the electrically conductive copper shunts, the typical ceramic plates and heat sinks. Therefore, keeping in mind the above salient points, a novel integrated TED structure is proposed, where a major part of the semiconductor material is replaced with a conductor, such as copper, along with flow channels drilled through it. This flow channel configuration acts as a low thermal resistance heat exchanger eliminating the thermal resistances attributed to the heat sinks. This novel design helps reduce thermal stresses, materials usage and the thermal resistances without compromising its conversion efficiencies and performance. In this paper, a fluid-thermo-electrically coupled three-dimensional numerical model for TEDs is implemented in the FLUENT-UDS package. Furthermore, using developed numerical model, the performance of such a novel integrated TED is investigated for different load circuitry resistance, hot fluid inlet temperature and flow rate values.

2. Geometry, Governing equations and Boundary conditions

The schematic of a novel integrated Thermoelectric Device (TED) with flow channel configuration being investigated is shown in Fig. 1. The integrated TED element with square cross-section $W \times D$ consists of a copper inter-connector laminated between crystalline n-type ($75\%\ Bi_2Te_3\ 25\%\ Bi_2Se_3$) and p-type ($25\%\ Bi_2Te_3\ 75\%\ Sb_2Te_3$, 1.75% excess Se) bulk materials. The inter-connector rectangular flow channel size is $0.8(L-2d)\times 0.6D$. The top and bottom surfaces of the TED element are connected to copper connectors. The end surfaces of these connectors act as electrical terminals for load circuitry of load resistance R_L. The top surface of the upper connector and bottom surface of the lower connector are subjected to constant cold temperature T_c. A hot fluid with constant temperature T_{in} and uniform velocity U_{in} enters the main flow channel of cross-sectional size $(L-2d)\times D$ at the inlet, flows the through inter-connector channel and leaves at the outlet (as shown in Fig. 1). The inter-connector left and right side surfaces and it's channel walls are exposed to the hot fluid. The remaining surfaces of TED and the main flow channel walls exposed to ambient are subjected to adiabatic condition.

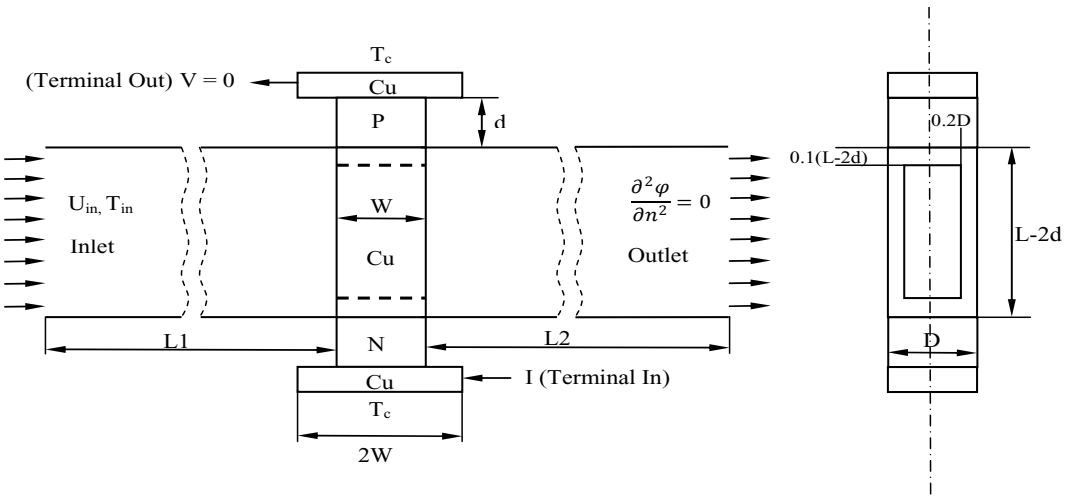

Fig. 1. Schematic of integrated thermoelectric device

The fluid flow and heat transport in the fluid domain are governed by the continuity of mass, momentum and energy equations subjected to certain assumptions. The flow is steady, laminar and incompressible. Thermo-physical properties of the fluid are invariant with temperature. In the thermoelectric material, the current flow and energy transport are governed by the continuity of current density and the energy equations subjected to following assumptions: the materials are heterogeneous and isotropic with temperature-dependent thermoelectric properties; electrical resistivity ρ, Seebeck coefficient α and thermal conductivity κ, are specified as polynomial functions of temperature [6]; the thermal and electrical contact resistances at the interface of n-type or p-type and copper materials are negligible. The system of partial differential equations governing the fluid-thermo-electric phenomenon in TEDs under steady-state conditions for the continuity, momentum and heat transport [1] is written as

For fluid domain: $$\nabla.\mathbf{v} = 0 \tag{1}$$

$$\rho_f(\mathbf{v}.\nabla\mathbf{v}) = -\nabla P + \mu\nabla^2\mathbf{v} \tag{2}$$

$$\rho_f c_p(\mathbf{v}.\nabla T) = \nabla.(k_f \nabla T) \tag{3}$$

For thermoelectric material: $$\nabla.\mathbf{J} = 0 \tag{4}$$

$$\nabla(\kappa\nabla T) + \rho\mathbf{J}^2 - T\mathbf{J}.\left[\left(\frac{\partial\alpha}{\partial T}\right)\nabla T + (\nabla\alpha)_T\right] = 0 \tag{5}$$

where $\mathbf{J}$ is the current density and it is evaluated as

$$\mathbf{J} = -\frac{1}{\rho}[\nabla V + \alpha\nabla T] = 0 \tag{6}$$

In Eq. (5), the second and third terms on the left-hand side represent the Joule heating, Peltier and Thomson effects respectively. In Eq. (6), the first and second terms on right-hand side are the current densities due to electrostatic potential distribution, and the Seebeck electric potential in the thermoelectric material, respectively.

The associated boundary conditions for Eqs. (1) to (6) with respect to the geometry shown in Fig. 1 are:

At the terminal in: $$\mathbf{J} = \frac{I}{A_\xi} = \frac{V_0}{A_\xi (R_{in} + R_L)} \qquad and \qquad \frac{\partial T}{\partial \xi} = 0 \tag{7}$$

where V_0 is the total build-in open circuit voltage generated in the element at a no-load condition, which is known as the Seebeck voltage. R_{in} is the total internal resistance equaling to the summation of n-type, p-type, connectors and inter-connector materials resistances and R_L represents the external load resistance.

At the terminal out: $$V = 0 \qquad and \qquad \frac{\partial T}{\partial \xi} = 0 \tag{8}$$

At the top wall of the upper connector and bottom wall of the lower connector:

$$T = T_c \qquad and \qquad \frac{\partial V}{\partial \xi} = 0 \tag{9}$$

All other surfaces of the TED are exposed to surroundings: $$\frac{\partial T}{\partial \xi} = 0 \qquad and \qquad \frac{\partial V}{\partial \xi} = 0 \tag{10}$$

At the fluid flow inlet: $x = 0$: $$u = U_{in}, v = w = 0 \qquad and \qquad T = T_{in} \tag{11}$$

At the fluid flow outlet: $x = (L1 + W + L2)$: $$\frac{\partial^2 u}{\partial \xi^2} = \frac{\partial^2 T}{\partial \xi^2} = v = w = 0 \tag{12}$$

At the channel walls exposed to surroundings: $$u = v = w = 0 \qquad and \qquad \frac{\partial T}{\partial \xi} = 0 \tag{13}$$

where ξ denotes the direction normal to the corresponding boundary wall. $L1$ = 5W and $L2$ = 20W are the lengths of the upstream and downstream boundaries of the TED, respectively (as shown in Fig. 1). At the interface between the n-type or p-type and conductor materials, the continuity of current density, temperature and heat flux conditions are imposed.

The power output from the TED for a given load resistance R_L, the total heat input at the inter-connector walls exposed to flowing fluid and the thermal conversion efficiency are evaluated as:

$$P_0 = I^2 R_L \qquad and \qquad Q_h = -k_f \int \frac{\partial T}{\partial \xi} dA_s \quad \eta = \frac{P_0}{Q_h} \tag{14}$$

3. Numerical solution methodology and validation

The numerical simulations are done using the finite volume formulation of Eqs. (1) to (5) and the associated constitutive relation (6) along with boundary conditions Eqs. (7) to (13) in ANSYS FLUENT-UDS (User Defined Scalar) environment. The integrated TED model and mesh are generated in Gambit 2.4. The pressure-velocity coupling is handled using SIMPLE algorithm. The convective term in Eq. (2), diffusion terms in Eqs. (2) and (4) and pressure term in Eq. (2) are descritized with a power law scheme. The Seebeck potential and Ohmic electric potential (Eq. (6)) are calculated using UDS fields. The Ohmic heating, Peltier and Thomson effects are modeled as source terms in the energy equation (Eq. (5)). The electric current is evaluated based on the open-circuit Seebeck voltage (V_0) produced at the given load resistance R_L (Eq. (7)). The detailed numerical implementation has been demonstrated in [5].

Table 1. Comparison of thermoelectric generator parameters $T_h = 427^\circ C$ and $T_c = 27^\circ C$

Quantity	Analytical [6]	ANSYS (a) [7]	ANSYS (b) [7]	Present (a)	Present (b)
Q_h, W	13.04	13.03	11.07	13.0	10.72
P_0, W	1.44	1.43	1.05	1.43	1.07
η, %	11	11	9.5	11	9.98
I, A	19.2	19.1	16.4	19.09	16.5

The convergence criteria (the difference between consecutive iterations over a domain) set for the flow is 10^{-4} and for the current density, energy, Seebeck and Ohmic electric potentials are 10^{-12} . Grid independence tests are performed for integrated TED (as shown in Fig. 1). A grid size 622800 of non-uniform, orthogonal grid used in the simulations. The developed three-dimensional thermoelectric numerical code has been validated with published results of a thermoelectric generator for the cases of (a) constant properties and (b) temperature-dependent properties as given in Table 1. The results are in good agreement with the published both analytical and numerical results.

4. Results and Discussion

The numerical simulations are conducted on a integrated thermoelectric device (TED) to study its performance when coupled with fluid flow phenomenon. The geometric dimensions i.e. cross-sectional area (W = 5 mm and D = 5 mm) and height (d = 5 mm) of the n or p-type element, the connector ($2W \times D \times 1.5$), the interconnector (((L-2d) $\times$ D) and its channel ($0.3D \times 0.8$(L-2d)) sizes are invariant. For fixed cold wall temperature T_c = 300 K, the performance of the TED in terms of the power output P_0, heat input Q_h, conversion efficiency η and Ohmic electric voltage V for various hot fluid inlet temperature $350 \le T_{in}(K) \le 550$, the load circuitry resistance $10^{-4} \le R_L(Ohms) \le 10^{-1}$ and the Reynolds number based on the hydraulic diameter D_h $50 \le Re_{Dh} \le 500$ has been investigated in detail.

4.1. Effects of load resistance R_L

For fixed $Re_{Dh} = 500$, Fig. 2 shows the variation of power output P_0, heat input Q_h, and conversion efficiency η and Ohmic voltage drop V with load resistance R_L for different inlet hot fluid temperatures T_{in} . From Figs. 2a and 2c, for a given T_{in} , there exists a maximum power output P_{0max} when R_L is equal to R_{in} and the TED has optimum thermal efficiency η at $R_L = R_{optmL}$, typically, which is not equal to R_{in} . The optimum load resistance R_{optmL} increases marginally with an increase in T_{in} values while all other are parameters kept constant. It is noticed that the R_{in} value is always slightly lesser than R_{optmL} for a given T_{in} condition. At higher T_{in} values, the increment in R_L showed significant variations in Q_h predictions, however, a minimal decrease at lower values of T_{in} is observed (in Fig. 2b).

From Fig. 2d, for a given T_{in} value, an increase in R_L results in a decrease in V values. This is due to the gain in total resistance $R_{in} + R_L$ value of the TED. On the other hand, at a given R_L value, an increment in T_{in} shows an enhancement in V values. This is due to raise in the Seebeck voltage through the temperature differential between the inter-connector channel wall and the cold surfaces $(T_h - T_c)$. Furthermore, irrespective of T_{in} value, the responses of V with R_L show same behaviour.

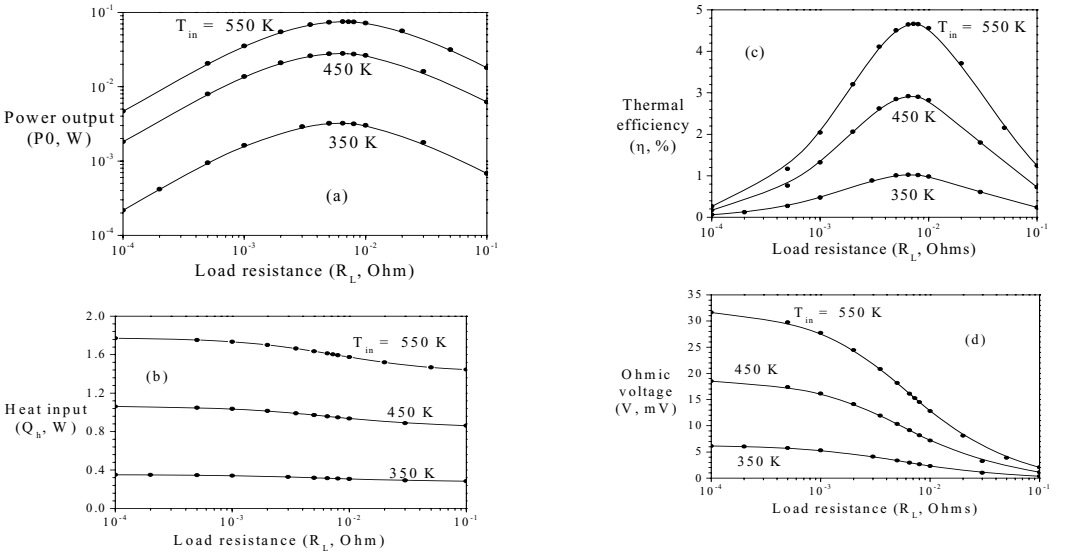

Fig. 2 The performance parameters variation with load resistance (R_L) (a) Electrical power output (b) Heat input (c) Thermal efficiency and (d) Ohmic voltage for various T_{in} values [at Re_{Dh} = 500, d = 5 mm, L = 20 mm, T_c = 300 K]

4.2. Effects of Reynolds number Re_{Dh}

Figures 3 and 4 show the performance of a integrated TED with Re_{Dh} values for different T_{in} values at optimum load resistance R_{optmL} conditions. For a fixed T_{in} , as the inlet flow rate Re_{Dh} increases, an enhancement in the performance parameters, namely P_0, Q_h, η and V , is observed. It indicates that the higher Re_{Dh} improves the heat transfer rate from inter-connector channel walls to TED, and hence, more temperature differential occurs between hot and cold end surfaces, which in turn produce a higher Seebeck voltage across the semiconductor elements. It is noticed that as T_{in} raises, the change in η with Re_{Dh} becomes prominent and the behaviour also reflects in P_0, Q_h, and V values. The reason could be the formation of recirculating zones near the inter-connector walls upstream and downstream of TED.

In Fig. 4a and b, represent the x-velocity and temperature contours with $T_{in} = 550K$ at the mid-plane (as shown in Fig. 1a) for Re_{Dh} = 50, 200 and 500 values, respectively. For clarity, a downstream length of $4W$ and a upstream length of $2.5W$ are only depicted in these figures. From the velocity contours, in the

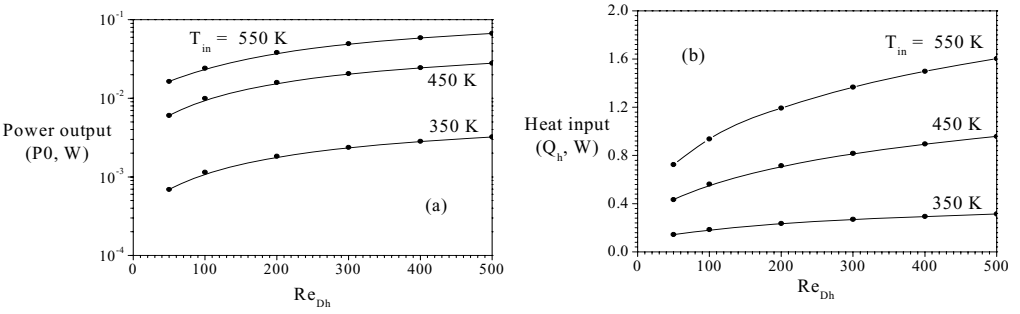

* Corresponding author. Tel.: +1-412-624-9720 fax: +1-412-624-4846.
E-mail address: mkchyu@pitt.edu

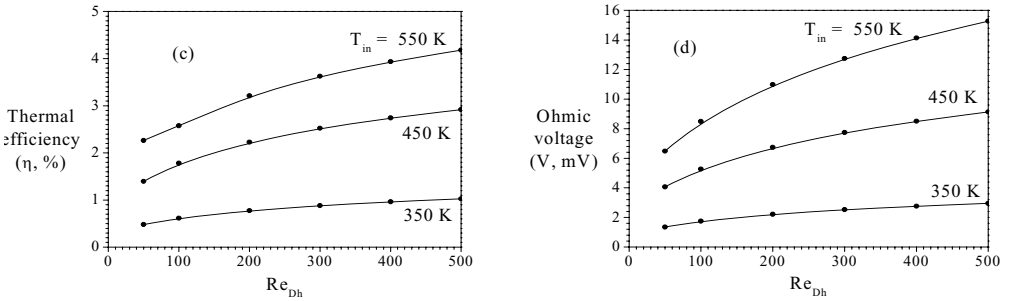

Fig. 3 The variation of (a) Electrical power output (b) Heat input (c) Thermal efficiency and (d) Ohmic voltage with Reynolds number (Re_{Dh} for different T_{in} values at R_{optm} values [at d = 5 mm, L = 20 mm, T_c = 300 K]

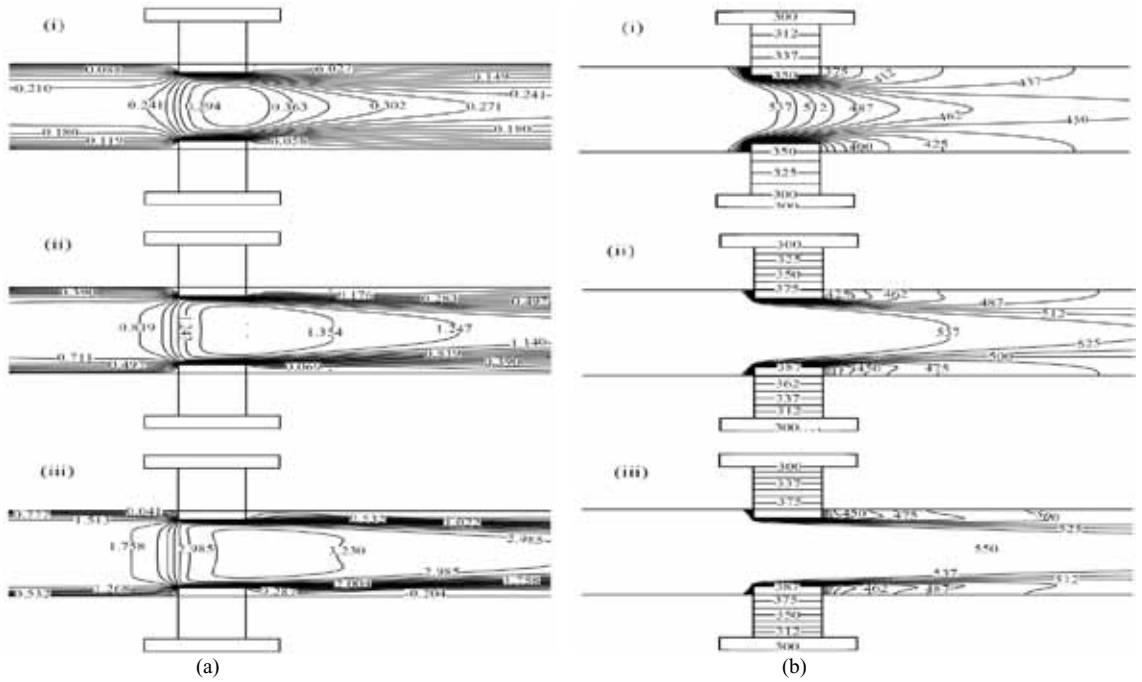

Fig. 4 The distribution of (a) x-velocity and (b) temperature on the depth-mid-plane at different Re_{Dh} values (i) 50 (ii) 200 and (iii) 500 [at T_{in} = 550 K, d = 5 mm, L = 20 mm, T_c = 300 K and R_{optm} = 6.5 × 10^{-3}]

downstream, it is seen that the flow accelerating towards the channel walls increases as the inlet flow Re_{Dh} raises. This flow behaviour helps in the enhancement of heat transfer due to the formation of the recirculation zones near inter-connector side walls. This trend has been revealed through raise in the inter-connector channel walls temperature as shown in Fig. 4b. The larger temperature gradients in the thermoelectric materials facilitate higher P_0 values (as shown in Fig. 3a).

5. Conclusions

The fluid-thermo-electric coupling mechanisms such as the Joule heating, Seebeck and Peltier effects, Thomson cooling/heating and convective heat transfer in thermoelectric devices(TEDs), along with

temperature-dependent material properties has been implemented in a FLUENT-UDS environment. By focusing on improvement in power output, minimization of thermal stresses and resistances, and reducing the usage of rare-earth materials in TED, without compromising its efficiency, a novel integrated TED has been proposed. The thermoelectric performance of such a device applied to waste heat recovery in terms of power out P_0, heat input Q_h, conversion efficiency η and Ohmic voltage V has been investigated using numerical simulations.

For a fixed inlet flow rate Re_{Dh} and fluid temperature T_{in}, the change in load resistance R_L results in an optimum conversion efficiency η and maximum power output P_{0max} at R_L equaling to the total internal resistance R_{in} and R_L equaling to the optimum load resistance R_{optmL}, respectively. The R_{optmL} increases marginally with an increase in T_{in} values is noticed when all other parameters kept constant. Simultaneously, a decrease in V values with raise in R_L values is observed.

For a given R_L value, an increment in T_{in} shows an enhancement in TED performance. It is also observed that at higher T_{in} values, the increment in R_L showed a significant change in Q_h predictions, however, a marginal decrease at lower values of T_{in}.

The higher flow rate Re_{Dh} enhances the heat transfer from the inter-connector channel walls of the TED, and hence produces a higher P_0. The formation of recirculation zones in the upstream and downstream of TED assist in heat transfer Q_h enhancement with an increase in T_{in}. Therefore, the fluid-thermo-electrical coupling phenomenon should be considered for detailed analysis of TED performance.

References

[1] Rowe DM. Thermoelectrics Handbook Macro to Nano. CRC Press, Taylor & Francis Group:Boca Raton; 2006.

[2] Caillat T, Fleurial JP, Snyder GJ, Zoltan A, Zoltan D, Borshchevsky A. Development of a high efficiency thermoelectricunicouple for power generation applications. In: Proc. XVllI Int. Conference on Thermoelectrics, Baltimore, USA, 1999.

[3] Hsiao Y, Chang W, Chen S. A mathematic model of thermoelectric module with applications on waste heat recovery from automobile engine, Energy 2010; 35:1447-1454.

[4] Kousksou T, Bdcarrats JP, Champier D, Pignolet P, Brillet C. Numerical study of thermoelectric power generation for an helicopter conical nozzle. J Power Sources 2011;196:4026-4032.

[5] Chen M, Rosendahl LA, Condra T. A three-dimensional numerical model of thermoelectric generators in uid power systems. Int.J Heat Mass Transfer 2011; 54:345-355.

[6] Angrist SW. Direct Energy Conversion. 4th ed. Boston: Allyn and Bacon; 1982.

[7] Antonova EE, Looman DC. Finite elements for thermoelectric device analysis in ansys, In:Int. Conference on Thermoelectrics, IEEE,2005, p. 200-203.